Amyloid, March 2006; 13(1): 1–5

Taylor & Francis
Taylor & Francis Group

Three-repeat Tau 69 is a major tau isoform in laser-microdissected Pick bodies

TAKUYA OHKUBO[1,2], YUJI SAKASEGAWA[3], HIROYUKI TODA[4], HITARU KISHIDA[4], KUNIMASA ARIMA[5], MITSUNORI YAMADA[6], HITOSHI TAKAHASHI[6], HIDEHIRO MIZUSAWA[2], NAOMI S. HACHIYA[1], & KIYOTOSHI KANEKO[1]

[1]*Second Department of Physiology, Tokyo Medical University, Tokyo, Japan,* [2]*Department of Neurology and Neurological Science, Graduate School of Medicine, Tokyo Medical and Dental University, Tokyo, Japan,* [3]*Department of Prion Protein Research, Tohoku University, Sendai, Japan,* [4]*Department of Neurology, Yokohama City University School of Medicine, Yokohama, Japan,* [5]*Department of Laboratory Medicine, National Center Hospital for Mental Nervous and Muscular Disorders, National Center of Neurology and Psychiatry, Tokyo, Japan, and* [6]*Department of Pathology, Brain Research Institute, Niigata University, Niigata, Japan*

Keywords: *Pick's disease, Pick body, Laser Microdissection System, phosphorylated tau, Tau 60, Tau 64, Tau 69*

Abbreviations: *LMDS-WB = Laser Microdissection System and Western blot analysis; PB = Pick body*

Abstract

By utilizing a novel combinatorial method of a Laser Microdissection System and Western blot analysis, we demonstrate that a distinct isoform of abnormally phosphorylated tau (69 kDa, Tau 69) predominantly aggregated in laser-microdissected Pick bodies (PBs) in sporadic Pick's disease. By contrast, tau migrated as two major bands of 60 and 64 kDa (Tau 60 and 64) in total brain homogenates as previously reported. Comparative immunohistochemical analysis with anti–4-repeat antibody revealed that a major component of the abnormally phosphorylated tau in these PBs was 3-repeat tau (3R-tau). Whether 29 amino acid repeat encoded by exons 2 and 3 in the Tau 69 might accelerate the formation of PBs remains to be further investigated. Such a combination of morphological and biochemical techniques significantly complements the existing histopathological methods.

Introduction

Pick's disease is a type of progressive presenile dementia, characterized by a frontotemporal cortical atrophy, widespread white matter degeneration and intraneuronal lesions denoted as Pick bodies (PBs), of which the major structural components are tau proteins. Abnormally phorphorylated tau proteins have been investigated by classical biochemical methods, and tau doublet (Tau 60 and Tau 64) was detected from brain homogenates in these patients [1–3] but not detected from normal brain homogenates, because tau proteins are not abnormally phosphorylated in normal brain [4].

Here we established a novel combinatorial method of a Laser Microdissection System [5] and Western blot analysis (LMDS-WB) which enables us to examine the molecular profile of proteins in microscopic regions of interest. Hence, we applied this novel method to examine PBs in Pick's disease, a sporadic tauopathy of progressive presenile dementia [6]. Subsequently, we identified a distinct pattern of tau isoforms in the laser-microdissected PBs, which was clearly different from those detected in total brain homogenates. These data suggest that a novel tau region is associated with the formation of PBs, other than the microtubule-binding motifs, in sporadic Pick's disease.

Materials and methods

Patients

Temporal cortexes from 2 patients with sporadic Pick's disease (patient 1 [sPiD1]; female, 55 years and patient 2 [sPiD2]; female, 76 years) were obtained from the National Center of Neurology and Psychiatry, Brain Research Institute, Niigata University. The sPiD1 was previously reported as

Correspondence: Dr Kiyotoshi Kaneko, Second Department of Physiology, Tokyo Medical University, 6-1-1 Shinjuku, Shinjuku-ku, Tokyo 160-8402, Japan. Tel: 81 3 3351 6141. ext. 322. Fax: 81 3 3351 6544. E-mail: k-kaneko@tokyo-med.ac.jp

The first two authors have equal contribution in this work and both are equally considered as "first author".

ISSN 1350-6129 print/ISSN 1744-2818 online © 2006 Taylor & Francis
DOI: 10.1080/13506120500535586

case 5 [7], and sPiD2 was also reported as case 2 [8]. The tissue was placed directly in a deep freezer at −80°C (sPiD1), or immediately quick-frozen in cold isopentane and kept in a deep freezer at −80°C (sPiD2) until use.

Laser-microdissection and Western blot analysis

The slide preparations for microbiochemical analysis were made by NexES® Automated Immunohistochemistry Staining System (Ventana Medical Systems, Inc., Tucson, AZ, USA). Immunostained solid samples of smaller than 10 μm^3 (Figure 1A) were dissected by our new Laser Microdissection System (Olympus Optical Co., ltd., Tokyo, Japan) coupled to HOYA laser cutter, HCL2100 (30 mJ/pulse, 266 nm, Hoya Co., Tokyo, Japan). Dissected samples were collected by the CellTram Oil®, hydraulic manual microinjector (Eppendorf, Hamburg, Germany) with distilled water. About 500 PBs were collected and analyzed each time (Figure 1B). Total brain homogenates (10 μg), laser-dissected PBs (500 pieces), and their surrounding brain tissues without PBs were solubilized in 500 μl of ice-cold

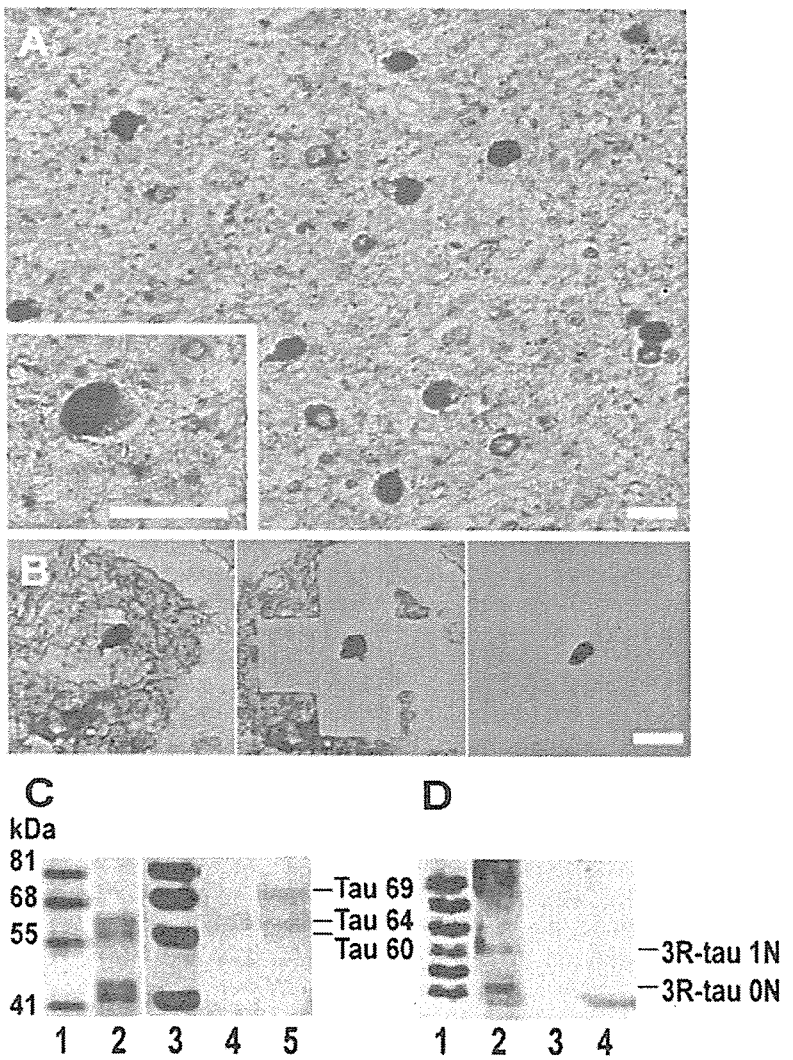

Figure 1. Temporal cortex, patient 1 with sporadic Pick's disease (sPiD1). (A) Ten-μm-thick cryosection. Pick bodies (PBs) of sPiD1 stained with AT8 (purple) and hematoxylin (blue). Scale bar is 20 μm. (B) Two-μm-thick cryosection of sPiD1. PBs isolated from the section by the Laser Microdissection System. Scale bar is 20 μm. (C) Western blot analysis of sPiD1 with AT8 and AT100 antibodies. Molecular weight marker (Dr. Western, Oriental Yeast, Tokyo, Japan, lanes 1 and 3), temporal brain homogenates (40 μg, lane 2), surrounding area of PBs (1–3 ng, lane 4), laser microdissected PBs (1–3 ng, lane 5). (D) Western blot analysis of sarkosyl-insoluble fraction of temporal brain homogenates of sPiD1 after dephosphorylation by bacterial alkaline phosphatase (8 μg, lane 2), blank lane (lane 3), and bacterial alkaline phosphatase alone (lane 4) with HT7 antibody. Molecular weight marker (six recombinant tau isoforms in lane 1; 67, 62, 59, 54, 52, and 48 kDa, respectively).

extraction buffer (Tris-chrolide (pH 7.4), 0.8 M NaCl, 1 mM EGTA, 10% sucrose and 1/1,000 w/v protease inhibitor cocktail (Sigma) with 1% sodium *N*-lauroyl sarcosinate. Sarkosyl-insoluble fractions were collected by 182,000 × *g* for 30 min at 4°C, and suspended in 50 mM Tris-chrolide (pH 7.4). The sarkosyl-insoluble material was boiled with Lammeli's buffer for 10 min at 95°C, loaded onto 12% SDS-PAGE gels and transferred onto nitrocellulose membranes. Nitrocellulose membranes were blocked with 5% non-fat milk in PBS-T and incubated with 1:1,000 AT100 (Innogenetics, Ghent, Belgium) specific to phosphorylated Thr 212/Ser 214, and 1:1,000 AT8 (Innogenetics, Ghent, Belgium) specific to phosphorylated Ser 202/Thr 205 of tau in PBS-T. Immunodecorated bands were visualized by SuperSignal West Femto Maximum Sensitivity Substrate (Pierce, Rockford, IL, USA), and analyzed using the Fluor-S MAX MultiImager or VersaDoc (Bio-Rad Laboratories, Hercules, CA, USA).

Sarkosyl-insoluble fraction of brain samples and their dephosphorylation

Frozen total brain sample (0.2 g) was homogenated with 500 μl of ice-cold extraction buffer (50 mM Tris-chrolide [pH 7.4], 0.8 M NaCl, 1 mM EGTA, 10% sucrose and 1/1,000 w/v protease inhibitor cocktail (Sigma)) and 1/10 volume of glassbeads. After 20,000 × *g* centrifugation for 10 min at 4°C, the supernatant was incubated with 1% sodium *N*-lauroyl sarcosinate. Sarkosyl-insoluble fractions were collected by 182,000 × *g* for 30 min at 4°C, and half of the sarkosyl-insoluble material was suspended in 50 mM Tris-chrolide (pH 7.4) for Western blot analysis of total brain sample [9].

The other half of the sarkosyl-insoluble material was used for the following dephosphorylation study. The sample was treated with 4 M guanidine hydrochloride for 1 h at room temperature, followed by overnight dialysis at 4°C against 50 mM Tris-chrolide (pH 8.8), 0.1 mM EDTA and 0.1 mM phenylmethylsulfonyl fluoride (PMSF). The sample was then incubated for 4 h at 67°C with 5 U/ml *E. coli* alkaline phosphatase (type III-N; Sigma). The incubated sample was purified with 1.5 M ammonium sulfate soloution to remove alkaline phosphatase for 1 h at room temperature. After 20,000 × *g* centrifugation for 10 min at 4°C, the pellet was suspended in 50 mM Tris-chrolide (pH 8.8) and boiled for 10 min at 95°C. The sample was then loaded onto 7.5% SDS-PAGE gels and transferred onto nitrocellulose membranes. Nitrocellulose membranes were blocked with 5% non-fat milk in phosphate buffered saline containing 0.05% Tween-20 (PBS-T) and incubated with 1:10,000 HT7 (Innogenetics, Ghent, Belgium) specific to amino acid residues 159–163 of tau in PBS-T. Immunodecorated bands were incubated with 1:10,000 horseradish peroxidase-cojugated anti-mouse IgG antibody in PBS-T, visualized by ECL plus, and analyzed using the VersaDoc.

Construction, expression, and purification of 6 recombinant tau isoforms

The classical Goedert's method [9] was modified as follows. Human full-length cDNA clones encoding six human tau protein isoforms were subcloned into the *Eco*RI site and *Xho*I site of pBluescript II SK+. Following cleavage with *Eco*RI and *Xho*I, the resulting cDNA fragments were subcloned downstream of the T7 RNA polymerase promoter into *Eco*RI and *Xho*I cut expression plasmid pET11a and the recombinant plasmids were transformed into *E. coli* BL21 (DE3) cells. The *E. coli* cells were grown to an optical density of 0.6–1.0 at 600 nm. Expression was induced by adding IPTG to a final concentration of 0.4 mM. After shaking for 3 h at 30°C, the cells were collected by centrifugation. The *E. coli* pellets were suspended in 50 mM PIPES (pH 6.8), 1 mM DTT, 1 mM EDTA and protease inhibitors cocktail (Sigma) and sonicated 1 × 10 min on ice using Branson Sonifier 250. The homogenates were centrifuged at 182,000 × *g* for 30 min at 4°C and the resultant supernatant was loaded onto a phosphocellulose packed column equibrated in extraction buffer.

After exhaustively washing in the same buffer, protein was eluted batchwise with 3 ml aliquots of extraction buffer containing 0.5 M NaCl. Fractions 2 and 3, which contained the recombinant tau proteins, were pooled and precipitated with 1.5 M ammonium sulfate. The pellet was washed in 50 mM PIPES (pH 6.8), 1 mM DTT, 1 mM EDTA and protease inhibitors cocktail (Sigma), and dialyzed overnight against 50 mM MES and 1 mM DTT (pH 6.5). After centrifugation the dialysate was loaded onto a Mono S HR 5/5 column (Amersham Biosciences). The column was washed with 50 mM MES, 1 mM DTT and 50 mM NaCl (pH 6.5), then the protein was eluted using a 100–300 mM NaCl gradient in 50 mM MES and 1 mM DTT (pH 6.5). Column fractions were screened by gel electrophoresis and Quick-CBB (Coomassie Brilliant Blue) PLUS stain (Wako), the peak tau fractions were pooled. Those fractions were then loaded onto a Superdex 200 HR 10/30 column (Amersham Biosciences). The column was washed with 50 mM MES, 1 mM DTT and 150 mM NaCl (pH 6.5). After screening column fractions by the same methods as above, the peak tau fractions were pooled, freezed by liquid nitrogen and stored in deep-freezer until use. After six tau isoforms

were collectively purified and measured their concentration with densitometry against bovine serum albumin, an equal volume of each of the six tau isoforms were mixed together. Five μl of this mixture were run alongside dephosphorylated sample for the molecular weight marker (Figure 1D).

Immunohistochemistry

Cryostat sections (2–20 μm thick) were made from the frozen material, fixed with cold acetone (−20°C) for 7 min, and immunostained by the avidin-biotin-peroxidase complex (ABC) method with a VECTASTATIN ABC elite kit (Vector Laboratories, Burlingame, CA, USA), using a mouse monoclonal antibody against phosphorylation-dependent tau proteins (AT8; Innogenetics, Ghent, Belgium, 1:200) or a rabbit antiserum against 4-repeat tau (4R-tau) (EX10; 1:2,000, kindly provided by Dr. T. Arai) [2]. For the later immunostaining, tissue sections were pretreated with 99% formic acid for 5 s. Diaminobenzidine was used as the chromogen. After immunostaining, the sections were counterstained with hematoxylin. For negative controls, the first antibodies were omitted or replaced with normal serum.

Results

In total brain homogenates of sPiD1, tau migrated as two major bands of 60 and 64 kDa (Tau 60 and 64) by common microgram scale Western blot (Figure 1C, lane 2) as previously described [1,2]. After dephosphorylation by bacterial alkaline phosphatase (type III-N; Sigma), tau in sarkosyl-insoluble fractions appeared as two major bands that align with either 3-repeat tau (3R-tau) 0N; 3R-tau with no N-terminal amino acids inserts (dephosphorylated Tau 60), or 3R-tau 1N; 3R-tau with 29 amino acids inserts encoded by exon 2 (dephosphorylated Tau 64) [Figure 1D, lane 2].

On the other hand, tau migrated as a major band of 69 kDa (Tau 69) in laser microdissected PBs (Figure 1C, lane 5), and Tau 64 predominated in surrounding area of PBs (Figure 1C, lane 4). In order to clarify whether the Tau 69 in PBs was composed of either 3R-tau or 4R-tau, comparative immunohistochemical analysis with anti 4R-tau antibody (EX10) was performed, since EX10 was not sensitive enough for our nanogram scale Western blot analysis due to the lack of efficient immunoreactions (data not shown). Further, the amount of laser microdissected PBs was insufficient for the dephosphorylation procedure. Definite immunoreactivity for 4R-tau was barely detectable in a small population of PBs (less than 1% of the total PBs, Figure 2B), while AT8 (phosphorylation dependent anti-tau antibody)-immunohistochemistry revealed the presence of many immunoreactive PBs (Figure 2A). From these data, we concluded that a major component of PBs in these patients are 3R-tau with 58 amino acids inserts encoded by exons 2 and 3 (represented as Tau 69).

Discussion

One possible scenario drawn from our results is that the 29 amino acid repeat in exons 2 and 3 may have a higher tendency to form PBs in a repeat-number-dependent manner, which is independent from the well-known microtubules-binding regions where tau mutations tend to cluster [10]. In fact, King et al. [11] experimentally observed that polymerization of the intact tau molecule was facilitated by the amino acid sequences in exons 2 and 3. It was also seen that insoluble tau of 69 kDa (Tau 69) predominantly

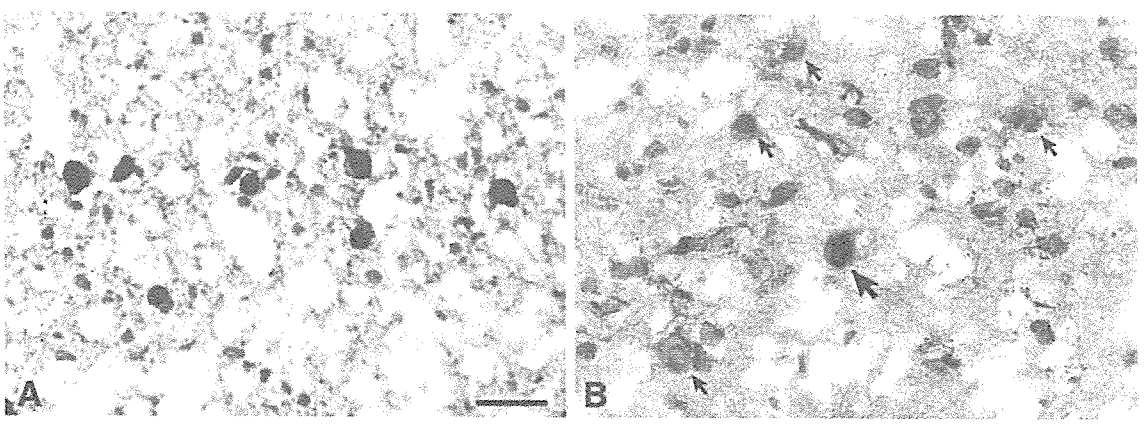

Figure 2. Immunoreactivity for phosphorylated tau (A) and 4R-tau (B) tau proteins in the second cortical layer of sPiD2. Intense labeling is present in many PBs in the panel A with AT8 antibody, but is restricted only in one PB in the panel B with EX10 antibody (large arrow). Small arrows in the panel B indicate PBs with little or no immunostaining. Scale bar is 30 μm.

accumulated in neuronal cells when normal human tau was expressed in *Caenorhabditis elegans* to model tauopathy disorders [12], which may further support our notion. Tau 69 is also observed in aggregates of other tauopathies including progressive supranuclear palsy (4R-tau) [2] and corticobasal degeneration (4R-tau) [2], or in Alzheimer's disease (3R and 4R-tau) [1]. Thus, such 29 amino acid repeats in exons 2 and 3 may also account for the formation of aggregates in these disorders.

As shown, both methods of immunohistochemistry and Western blot are mutually complementary at the microscopic level. Of note, our novel combination method (LMDS-WB) targets proteins in the specific regions of interest at the micrometer order, which was separated by SDS-PAGE and immunoblotted, and thus, exclusively enables us to gather information on the molecular profile (i.e. molecular weight) of target proteins under the microscope *in situ*. In fact, we successfully detected distinct isoforms of abnormally phosphorylated tau in PBs for the first time, something never observed from total brain homogenates with conventional approaches. However, immunohistochemistry usually exhibits a greater sensitivity compared to antibodies used for these purposes. For example, immunohistochemistry using AT8 was able to stain PBs at a single cell level, although at least a few hundred PBs were required for our combinatorial method of LMDS-WB with AT100.

Nonetheless, our method has indispensable advantages over the immunohistochemistry as shown in this study. Such a combination of morphological and biochemical techniques significantly complements the existing histopathologic methods, and has a great potential for investigating normal or abnormal microstructures in various conditions and disorders.

Acknowledgements

We thank K. Watanabe and K. Takayama for technical assistance. This work was supported by grants from the Ministry of Health, Labor and Welfare and the Ministry of Education, Culture, Sports, Science and Technology, Japan, and the Core Research for Evolutional Science and Technology (CREST) of Japan Science and Technology Agency.

References

1. Delacourte A, Sergeant N, Wattez A, Gauvreau D, Robitaille Y. Vulnerable neuronal subsets in Alzheimer's and Pick's disease are distinguished by their tau isoform distribution and phosphorylation. Ann Neurol 1998;43:193–204.
2. Arai T, Ikeda K, Akiyama H, Shikamoto Y, Tsuchiya K, Yagishita S, Beach T, Rogers J, Schwab C, McGeer PL. Distinct isoforms of tau aggregated in neurons and glial cells in brains of patients with Pick's disease, corticobasal degeneration and progressive supranuclear palsy. Acta Neuropathol (Berl) 2001;101:167–173.
3. Zhukareva V, Mann D, Pickering-Brown S, Uryu K, Shuck T, Shah K, Grossman M, Miller BL, Hulette CM, Feinstein SC, et al. Sporadic Pick's disease: a tauopathy characterized by a spectrum of pathological tau isoforms in gray and white matter. Ann Neurol 2002;51:730–739.
4. Sergeant N, Delacourte A, Buee L. Tau protein as a differential biomarker of tauopathies. Biochim Biophys Acta 2005;1739:179–197.
5. Tanaka T, Ito T, Furuta M, Eguchi C, Toda H, Wakabayashi-Takai E, Kaneko K. In Situ Phage Screening. A method for identification of subnanogram tissue components in situ. J Biol Chem 2002;277:30382–30387.
6. Buee L, Bussiere T, Buee-Scherrer V, Delacourte A, Hof PR. Tau protein isoforms, phosphorylation and role in neurodegenerative disorders. Brain Res Brain Res Rev 2000;33: 95–130.
7. Arima K. Involvement of subcortical nuclei and brain stem in Pick's disease: a topographical study of Pick bodies. Neuropathology 1989;9:105–115.
8. Mori F, Hayashi S, Yamagishi S, Yoshimoto M, Yagihashi S, Takahashi H, Wakabayashi K. Pick's disease: alpha- and beta-synuclein-immunoreactive Pick bodies in the dentate gyrus. Acta Neuropathol (Berl) 2002;104:455–461.
9. Goedert M, Spillantini MG, Cairns NJ, Crowther RA. Tau proteins of Alzheimer paired helical filaments: abnormal phosphorylation of all six brain isoforms. Neuron 1992;8: 159–168.
10. Lee VM, Goedert M, Trojanowski JQ. Neurodegenerative tauopathies. Annu Rev Neurosci 2001;24:1121–1159.
11. King ME, Gamblin TC, Kuret J, Binder LI. Differential assembly of human tau isoforms in the presence of arachidonic acid. J Neurochem 2000;74:1749–1757.
12. Kraemer BC, Zhang B, Leverenz JB, Thomas JH, Trojanowski JQ, Schellenberg GD. Neurodegeneration and defective neurotransmission in a Caenorhabditis elegans model of tauopathy. Proc Natl Acad Sci USA 2003;100: 9980–9985.

Medical Hypotheses (2007) 68, 670–673

ELSEVIER

medical hypotheses

http://intl.elsevierhealth.com/journals/mehy

The possible role of protein X, a putative auxiliary factor in pathological prion replication, in regulating a physiological endoproteolytic cleavage of cellular prion protein

Naomi S. Hachiya, Midori Imagawa, Kiyotoshi Kaneko *

Department of Neurophysiology, Tokyo Medical University, 6-1-1 Shinjuku, Tokyo 160-8402, Japan

Received 9 July 2006; accepted 19 July 2006

Summary The posttranslational conformational conversion of the cellular isoform of prion protein PrP^{C} into its scrapie isoform PrP^{Sc} is the fundamental process underlying the pathogenesis of prion disease. Based on several transgenic data, it has been postulated that a putative auxiliary factor denoted protein X functions as a molecular chaperone through its unfolding activity of PrP^{C} during the formation of PrP^{Sc}. However, the assumption that protein X therefore exists exclusively in prion diseases appears improbable and thus, it should have some simultaneous physiological role. We, hereby, propose a novel concept – a characteristic role of protein X in supporting a physiological endoproteolytic cleavage of PrP^{C}. The events corresponding to the formation of the physiologically metabolized PrP^{C} or the pathologically transformed PrP^{Sc} are mutually exclusive. Amino acid residues that are critical in terms of the target site of protein X for the pathological alteration into PrP^{Sc} overlap at the cleavage site. These amino acid residues tend to have a hydrophobic property and are most probably found buried inside the native protein structure. Therefore, a putative molecular chaperone identical to protein X may target the same hydrophobic residues in PrP^{C} and work in conjunction with either PrP^{Sc} in prion disease or PrP proteases during the physiological state. This postulation may help explain in a relatively simple manner these two mutually exclusive phenomena, viz. the physiological endoproteolytic cleavage of PrP^{C} and its pathological conversion into PrP^{Sc}.

The prion protein exists as two isoforms: a cellular isoform (PrP^{C}) that is rich in α-helices, and a disease (scrapie) isoform PrP^{Sc} that is rich in β-structures [1,2]. Many lines of evidence have predicated the persuasive argument that prions are composed largely, if not entirely, of the scrapie isoform [1]. After the synthesis of PrP^{C}, it is transited through the endoplasmic reticulum and Golgi apparatus to the cell surface where it is bound by a glycophosphatidyl inositol (GPI) anchor [3,4]. Subsequently, two mutually exclusive events take place – the metabolism of PrP^{C} and the conversion of PrP^{C} into PrP^{Sc} [5–7].

During the physiological event, the initial degradation of PrP^{C} involves endoproteolytic cleavage of

* Corresponding author. Tel.: +81 3 3351 6141x322; fax: +81 3 3351 6544.
E-mail address: k-kaneko@tokyo-med.ac.jp (K. Kaneko).

0306-9877/$ - see front matter © 2006 Elsevier Ltd. All rights reserved.
doi:10.1016/j.mehy.2006.07.038

the NH2-terminal fragment to produce a COOH-terminal polypeptide, which can be found in caveolae-like membrane domains or lipid rafts [5]. The NH2-terminal fragment of the PrP functions as a putative targeting element [8,9] and is essential for both its transport to the plasma membrane and the modulation of endocytosis [10]. A green fluorescent protein (GFP)-tagged version of PrP^C has been observed to be properly anchored to the cell surface; its distribution pattern has been reported to be similar to that of the endogenous PrP^C, and it has shown labeling at the plasma membrane and in intracellular perinuclear compartments [11–17].

This cleavage site is mapped to the amino acid residues between the anti-PrP 3F4 and anti-PrP 13A5 epitopes (amino acid 108/111 to amino acid 138 in mouse PrP) [5,18,19] (Fig. 1). It has also been reported that PrP^C cleavage occurs between amino acids 114 and 137 in chicken PrP [20] and between 110 and 113 in human PrP [21]. This proteolytic cleavage of PrP^C in the brain is blocked by metalloprotease inhibitors [22].

Other investigators have reported that PrP^C undergoes constitutive and phorbol ester-regulated cleavage. During such events, normal processing in human cells and murine neurons is upregulated by protein kinase C but not by protein kinase A [23]. Further experimentation indicated that a disintegrin and two metalloprotease family proteins, namely, ADAM10 and TACE, contribute to these cleavage reactions of PrP^C. ADAM10 contributes to the constitutive proteolytic cleavage of PrP^C, whereas TACE mainly participates in the regulated cleavage event [24].

The solution nuclear magnetic resonance (NMR) structure of monomeric recombinant PrP^C illustrates that this region is largely unstructured [25–27], whereas the crystal structure of the human prion protein in dimer form and that of the sheep prion protein suggest that this region is, at least in part, structured and organized [28,29]. Apart from these results with recombinant PrP, little is known about the endogenous native PrP^C conformation so far, except that these amino acid residues around the cleavage site have a hydrophobic property [30–32]; therefore, it is highly probable that they are buried within the native protein structure – a region that is barely accessible to the extrinsic proteases (Fig. 1) [33]. Thus, a putative molecular chaperone that should exhibit an unfolding activity on this hydrophobic region is expected to facilitate, at least to some extent, efficient PrP^C proteolysis through its physiological metabolic pathway.

This assumption is reminiscent of the concept that the association of protein X in prion replication with the pathological condition that is unidentified thus far [26,34,35]. The binding of PrP^C to protein X is accompanied by a conformational change (i.e., unfolding) in PrP^C, similar to that evident in the case of the molecular chaperone. This intermediate has been designated PrP^* [36]. The PrP^{Sc}/PrP^*/protein X complex is modulated by an undefined process, following which PrP^* is converted into PrP^{Sc} and protein X is released [37]. Interestingly, a prion-like protein in yeast, namely Sup35, apparently requires intermediate levels of the molecular chaperone Hsp104 to undergo transformation to [PSI^+] [38].

It is noteworthy that the amino acid residues that are critical in terms of the target site of protein X for the pathological conversion into PrP^{Sc} overlap at the physiological cleavage site where another putative molecular chaperone is expected to target and operate in conjunction with PrP proteases [2]. Hence, we can assume that these two putative molecules that exhibit a chaperone-like (i.e., unfolding) activity against the same hydrophobic residues in PrP^C could be identical. If we assume that the converse is true, then protein X exists exclusively for the pathological condition in terms of prion replication; this, however, appears to be less probable. Instead, our current hypothesis may lend a satisfactory explanation for these two mutually exclusive phenomena, i.e., physiological endoproteolytic cleavage of PrP^C and its pathological conversion into PrP^{Sc}. The identification of this putative molecular chaperone working in conjunction with proteases that target PrP^C is significant

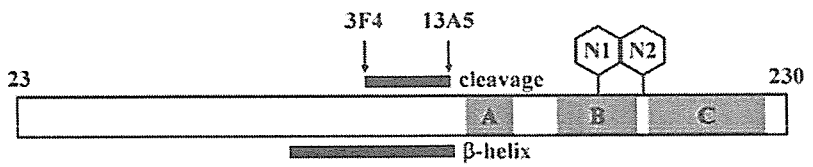

Figure 1 Endoproteolytic cleavage and pathological conversion into β-helix of the mouse cellular prion protein (Mo PrP^C). 3F4, anti-PrP 3F4 epitope (Mo 108/111); 13A5, anti-PrP13A5 epitope (Mo 138); A, helix A; B, helix B; C, helix C; N1 & N2, N-linked glycosylation sites (Mo 182/198); β-helix, β-helical region (Mo 90–140) of scrapie isoform of PrP (PrP^{Sc}); cleavage, mapped region of PrP^C cleavage site.

because it could also be also directed toward identifying protein X in prion replication – an issue that has not been elucidated for over a decade.

References

[1] Prusiner SB. Prions Proc Natl Acad Sci USA 1998;95: 13363–83.

[2] Wille H, Michelitsch MD, Guenebaut V, et al. Structural studies of the scrapie prion protein by electron crystallography. Proc Natl Acad Sci USA 2002;99:3563–8.

[3] Stahl N, Borchelt DR, Hsiao K, Prusiner SB. Scrapie prion protein contains a phosphatidylinositol glycolipid. Cell 1987;51:229–40.

[4] Caughey B, Race RE, Ernst D, Buchmeier MJ, Chesebro B. Prion protein biosynthesis in scrapie-infected and uninfected neuroblastoma cells. J Virol 1989;63:175–81.

[5] Taraboulos A, Scott M, Semenov A, et al. Cholesterol depletion and modification of COOH-terminal targeting sequence of the prion protein inhibit formation of the scrapie isoform. J Cell Biol 1995;129:121–32.

[6] Vey M, Pilkuhn S, Wille H, et al. Subcellular colocalization of the cellular and scrapie prion proteins in caveolae-like membranous domains. Proc Natl Acad Sci USA 1996;93: 14945–9.

[7] Kaneko K, Vey M, Scott M, et al. COOH-terminal sequence of the cellular prion protein directs subcellular trafficking and controls conversion into the scrapie isoform. Proc Natl Acad Sci USA 1997;94:2333–8.

[8] Shyng SL, Heuser JE, Harris DA. A glycolipid-anchored prion protein is endocytosed via clathrin-coated pits. J Cell Biol 1994;125:1239–50.

[9] Shyng SL, Moulder KL, Lesko A, Harris DA. The N-terminal domain of a glycolipid-anchored prion protein is essential for its endocytosis via clathrin-coated pits. J Biol Chem 1995;270:14793–800.

[10] Nunziante M, Gilch S, Schatzl HM. Essential role of the prion protein N terminus in subcellular trafficking and half-life of cellular prion protein. J Biol Chem 2003;278:3726–34.

[11] Lee KS, Magalhaes AC, Zanata SM, et al. Internalization of mammalian fluorescent cellular prion protein and N-terminal deletion mutants in living cells. J Neurochem 2001;79:79–87.

[12] Magalhaes AC, Silva JA, Lee KS, et al. Endocytic intermediates involved with the intracellular trafficking of a fluorescent cellular prion protein. J Biol Chem 2002;277: 33311–8.

[13] Negro A, Ballarin C, Bertoli A, Massimino ML, Sorgato MC. The metabolism and imaging in live cells of the bovine prion protein in its native form or carrying single amino acid substitutions. Mol Cell Neurosci 2001;17:521–38.

[14] Lorenz H, Windl O, Kretzschmar HA. Cellular phenotyping of secretory and nuclear prion proteins associated with inherited prion diseases. J Biol Chem 2002;277: 8508–16.

[15] Ivanova L, Barmada S, Kummer T, Harris DA. Mutant prion proteins are partially retained in the endoplasmic reticulum. J Biol Chem 2001;276:42409–21.

[16] Hachiya NS, Watanabe K, Sakasegawa Y, Kaneko K. Microtubules-associated intracellular localization of the NH(2)-terminal cellular prion protein fragment. Biochem Biophys Res Commun 2004;313:818–23.

[17] Hachiya NS, Watanabe K, Yamada M, Sakasegawa Y, Kaneko K. Anterograde and retrograde intracellular trafficking of fluorescent cellular prion protein. Biochem Biophys Res Commun 2004;315:802–7.

[18] Rogers M, Serban D, Gyuris T, et al. Epitope mapping of the Syrian hamster prion protein utilizing chimeric and mutant genes in a vaccinia virus expression system. J Immunol 1991;147:3568–74.

[19] Pan KM, Stahl N, Prusiner SB. Purification and properties of the cellular prion protein from Syrian hamster brain. Protein Sci 1992;1:1343–52.

[20] Harris DA, Huber MT, van Dijken P, et al. Processing of a cellular prion protein: identification of N- and C-terminal cleavage sites. Biochemistry 1993;32:1009–10016.

[21] Chen SG, Teplow DB, Parchi P, et al. Truncated forms of the human prion protein in normal brain and in prion diseases. J Biol Chem 1995;270:19173–80.

[22] Jimenez-Huete A, Lievens PM, Vidal R, et al. Endogenous proteolytic cleavage of normal and disease-associated isoforms of the human prion protein in neural and non-neural tissues. Am J Pathol 1998;153: 1561–72.

[23] Vincent B, Paitel E, Frobert Y, et al. Phorbol ester-regulated cleavage of normal prion protein in HEK293 human cells and murine neurons. J Biol Chem 2000;275:35612–6.

[24] Vincent B, Paitel E, Saftig P, et al. The disintegrins ADAM10 and TACE contribute to the constitutive and phorbol ester-regulated normal cleavage of the cellular prion protein. J Biol Chem 2001;276:37743–6.

[25] Donne DG, Viles JH, Groth D, et al. Structure of the recombinant full-length hamster prion protein PrP(29–231): the N terminus is highly flexible. Proc Natl Acad Sci USA 1997;94:13452–7.

[26] James TL, Liu H, Ulyanov NB, et al. Solution structure of a 142-residue recombinant prion protein corresponding to the infectious fragment of the scrapie isoform. Proc Natl Acad Sci USA 1997;94:10086–91.

[27] Zahn R, Liu A, Luhrs T, et al. NMR solution structure of the human prion protein. Proc Natl Acad Sci USA 2000;97:145–50.

[28] Knaus KJ, Morillas M, Swietnicki W, et al. Crystal structure of the human prion protein reveals a mechanism for oligomerization. Nat Struct Biol 2001;8:770–4.

[29] Haire LF, Whyte SM, Vasisht N, et al. The crystal structure of the globular domain of sheep prion protein. J Mol Biol 2004;336:1175–83.

[30] Pillot T, Lins L, Goethals M, et al. The 118–135 peptide of the human prion protein forms amyloid fibrils and induces liposome fusion. J Mol Biol 1997;274:381–93.

[31] Jobling MF, Stewart LR, White AR, et al. The hydrophobic core sequence modulates the neurotoxic and secondary structure properties of the prion peptide 106–126. J Neurochem 1999;73:1557–65.

[32] Saez-Cirion A, Nieva JL, Gallaher WR. The hydrophobic internal region of bovine prion protein shares structural and functional properties with HIV type 1 fusion peptide. AIDS Res Hum Retroviruses 2003;19:969–78.

[33] Kaneko K, Hachiya NS. The alternative role of 14-3-3 zeta as a sweeper of misfolded proteins in disease conditions. Med Hypotheses 2006;67:169–71.

[34] Telling GC, Scott M, Mastrianni J, et al. Prion propagation in mice expressing human and chimeric PrP transgenes implicates the interaction of cellular PrP with another protein. Cell 1995;83:79–90.

[35] Kaneko K, Zulianello L, Scott M, et al. Evidence for protein X binding to a discontinuous epitope on the cellular prion protein during scrapie prion propagation. Proc Natl Acad Sci USA 1997;94:10069–74.

[36] Cohen FE, Prusiner SB. Pathologic conformations of prion proteins. Annu Rev Biochem 1998;67:793–819.
[37] Prusiner SB, Scott MR, DeArmond SJ, Cohen FE. Prion protein biology. Cell 1998;93:337–48.
[38] Chernoff YO, Lindquist SL, Ono B, Inge-Vechtomov SG, Liebman SW. Role of the chaperone protein Hsp104 in propagation of the yeast prion-like factor [*psi*⁻]. Science 1995;268:880–4.

ELSEVIER

Cell Biology International 30 (2006) 952–956

Cell Biology International

www.elsevier.com/locate/cellbi

Short communication

Gene silencing analyses against *amyloid precursor protein* (*APP*) gene family by RNA interference

Tokiko Sakai [a,b], Hirohiko Hohjoh [a,*]

[a] *National Institute of Neuroscience, National Center of Neurology and Psychiatry, 4-1-1 Ogawahigashi, Kodaira, Tokyo 187-8502, Japan*
[b] *Central Research Laboratories, Seikagaku Corporation, Tokyo, Japan*

Received 28 March 2006; revised 3 June 2006; accepted 26 June 2006

Abstract

Amyloid precursor protein (*APP*) and *amyloid precursor-like proteins 1* and *2* (*APLP1* and *APLP2*) are members of a large gene family. Although APP is known to be the source of the β-amyloid peptides involved in the development of Alzheimer's disease, the normal functions of APP, APLP1 and APLP2 in cells are poorly understood. In this study, we carried out gene silencing analysis by means of RNA interference with synthetic small interfering RNA duplexes targeting the *App*, *Aplp1* and *Aplp2* genes in Neuro2a (N2a) cells, a mouse neuroblastoma cell line. The results demonstrated that cell viability and neurite outgrowth of N2a cells undergoing knockdown of *Aplp1* were significantly reduced, compared with N2a cells undergoing knockdown of either *App* or *Aplp2*.

Keywords: RNAi; App; Aplp1; Aplp2; Neuro2a cell; Neurite outgrowth; Viability

1. Introduction

Amyloid precursor protein (APP) is a membrane-spanning glycoprotein expressed in various tissues, including the brain, and is the source of β-amyloid peptides (Aβ), which are a key factor in the development of Alzheimer's disease (AD); extracellular deposition of Aβ resulting in the formation of 'senile plaques' often occurring in the brains of AD patients (Turner et al., 2003). In mammals, *amyloid precursor-like protein 1* and *2* (*APLP1* and *APLP2*) genes, which lack the Aβ region, have also been identified (Wasco et al., 1992; Wasco et al., 1993a,b), thus suggesting that *APP*, *APLP1* and *APLP2* are members of a large gene family. The expression profiles of *APP* and *APLP2* are similar, whereas expression of *APLP1* appears to be restricted to the nervous system (Lorent et al., 1995; Slunt et al., 1994). Translated APP, APLP1 and APLP2 polypeptides appear to undergo proteolytic processing by α-, β- and γ-secretase (Eggert et al., 2004; Gu et al., 2001; Li and Sudhof, 2004; Scheinfeld et al., 2002); but, the normal function of the resultant APP, APLP1 and APLP2 in cells remains largely unknown.

In this study, we carried out gene silencing analysis against the *App*, *Aplp1* and *Aplp2* genes by means of RNA interference (RNAi) in Neuro2a (N2a) cells, a mouse neuroblastoma cell line, and investigated the influence of knockdown of these genes.

2. Materials and methods

2.1. Cell culture

Neuro2a cells, a mouse neuroblastoma cell line, were grown at 37 °C in DMEM (Wako) supplemented with 10% fetal bovine serum (Sigma), 100 U/ml penicillin (Invitrogen) and 100 μg/ml streptomycin (Invitrogen) in a 5% CO_2-humidified chamber.

2.2. Small interfering RNA duplexes

Small interfering RNA (siRNA) duplexes against mouse *App*, *Aplp1*, and *Aplp2* genes were purchased from Ambion. The siRNA ID numbers (Ambion)

* Corresponding author. Tel.: +81 42 341 2711x5951; fax: +81 42 346 1755.
E-mail address: hohjohh@ncnp.go.jp (H. Hohjoh).

1065-6995/$ - see front matter © 2006 International Federation for Cell Biology. Published by Elsevier Ltd. All rights reserved.
doi:10.1016/j.cellbi.2006.06.018

were as follows: siApp-1 [60001], siApp-2 [60093], siAplp1-1 [159681], siAplp1-2 [159682], siAplp2-1 [160719], siAplp2-2 [160720]. Non-silencing siRNA duplexes were used as negative control (Qiagen).

2.3. Transfection of siRNA duplexes

The day before transfection, cells were trypsinized, diluted with fresh medium lacking antibiotics, and seeded into 24-well culture plates (1×10^4 cells/well). Transfection of siRNA duplexes was carried out using jetSI (Polyplus transfection) according to the manufacturer's instructions, with minor modifications. Before transfection, the culture medium was replaced with 0.4 ml OPTI-MEM I (Invitrogen), and to each well, 40 nM siRNA duplex was applied. Cells were incubated for 4 h at 37 °C. After the 4 h incubation, 1 ml of the fresh culture medium without antibiotics was added, and further incubation was carried out.

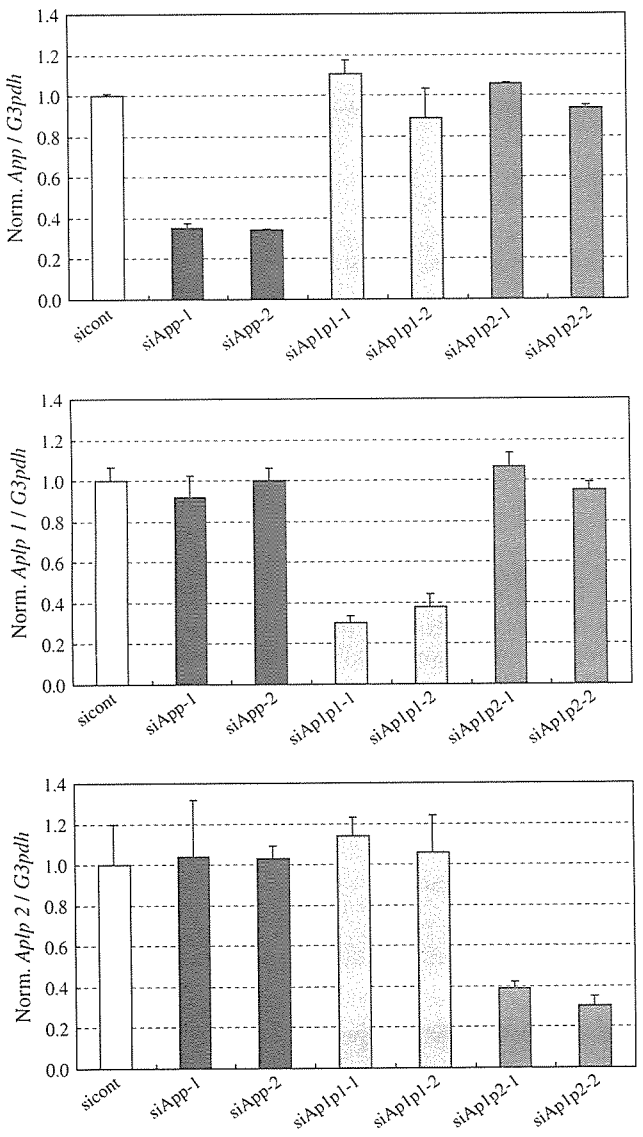

Fig. 1. Expression profiles of *App*, *Aplp1* and *Aplp2* in N2a cells. Indicated siRNA duplexes were transfected into N2a cells. Twelve hours after transfection, total RNA was extracted from the cells, and was subjected to RT-(real-time) PCR. Expression levels of *App*, *Aplp1*, or *Aplp2* were normalized against those of *G3pdh*, and the ratios of expression levels were normalized against the ratio obtained in the presence of the siControl duplex. Data are means of at least three independent determinations. Error bars represent standard deviations.

2.4. Reverse transcription-(real-time) polymerase chain reaction

In order to examine the expression levels of the genes, total RNA was extracted from cells and was subjected to reverse transcription-(real-time) polymerase chain reaction [RT-(real-time) PCR], as described previously (Hohjoh, 2004; Ohnishi et al., 2006; Sago et al., 2004). Real-time PCR was carried out using the ABI PRISM 7300 sequence detection system (Applied Biosystems) with a TaqMan Universal PCR Master Mix together with Assays-on-Demand Gene Expression products (Applied Biosystems) according to the manufacturer's instructions. The Assays-on-Demand Gene Expression products used (Assay ID number) were as follows: *App*; Mm00431827_m1, Aplp1; Mm00545893_m1, Aplp2; Mm00507819_m1.

2.5. Western blotting

Cell lysate and culture media were examined by Western blotting as described previously (Ohnishi et al., 2006). Equal amounts of proteins were separated by SDS-PAGE and electrophoretically blotted onto PVDF membranes (Millipore). Membranes were blocked with 5% non-fat milk in PBS containing 0.05% Tween-20 and incubated with anti-APP mouse monoclonal (3E9) antibody (MBL), anti-APLP1 rabbit polyclonal antibody (Calbiochem) and anti-α-tubulin (Sigma) antibody followed by washing in PBS and further incubation with horseradish peroxidase-conjugated anti-mouse IgG (Jackson ImmunoResearch Labs) or biotinylated anti-rabbit IgG together with avidin–biotinylated horseradish peroxidase complexes (Vectastain). Antigen–antibody complexes were visualized using ECL chemiluminescent reagent (Amersham).

2.6. Cell viability assay

Cell viability was investigated using 3-(4,5-dimethylthiazol-2-yl)-5(3-carboxymethonyphenol)-2-(4-sulfophenyl)-2*H*-tetrazolium (MTS) assay using a CellTiter 96 aqueous non-radioactive cell proliferation assay kit (Promega) according to the manufacturer's instructions.

3. Results and discussion

Because the *App*, *Aplp1* and *Aplp2* genes are members of the same gene family, we first assessed whether sequence-specific

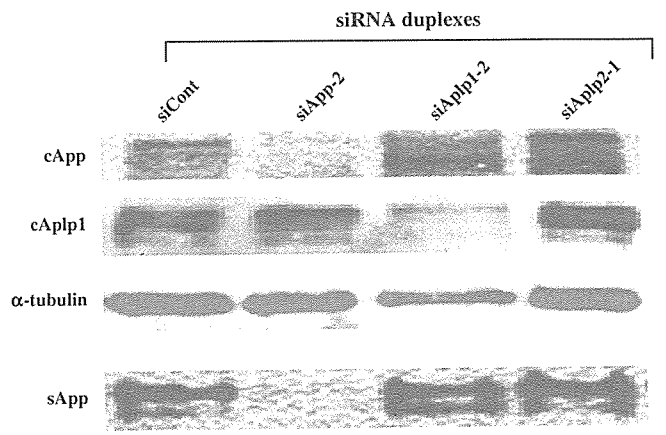

Fig. 2. Western blot analysis of App and Aplp1. Transfection of indicated siRNA duplexes into N2a cells was carried out as described for Fig. 1. Twenty-four hours after transfection, culture medium was replaced with DMEM without serum, and further 24 h culture was carried out. Cell lysate and culture media were prepared from transfected cells, and expressed App and Aplp1 in cells (cellular App and Aplp1: cApp and cAplp1) and App in culture media (secreted App: sApp) were examined by Western blotting. Expression of α-tubulin (control) was also examined. As for Aplp2, we could not obtain antibody against it in this study.

gene silencing (RNAi) was induced by siRNA duplexes. Twelve hours after transfection with the siRNA duplexes targeting *App*, *Aplp1* and *Aplp2*, the expression levels of the target genes were examined by means of RT-(real-time) PCR and Western blotting. As shown in Figs. 1 and 2, the results indicate that used siRNA duplexes were able to inhibit the expression of their own target genes without suppressing the expression of the other two genes, thus suggesting that specific

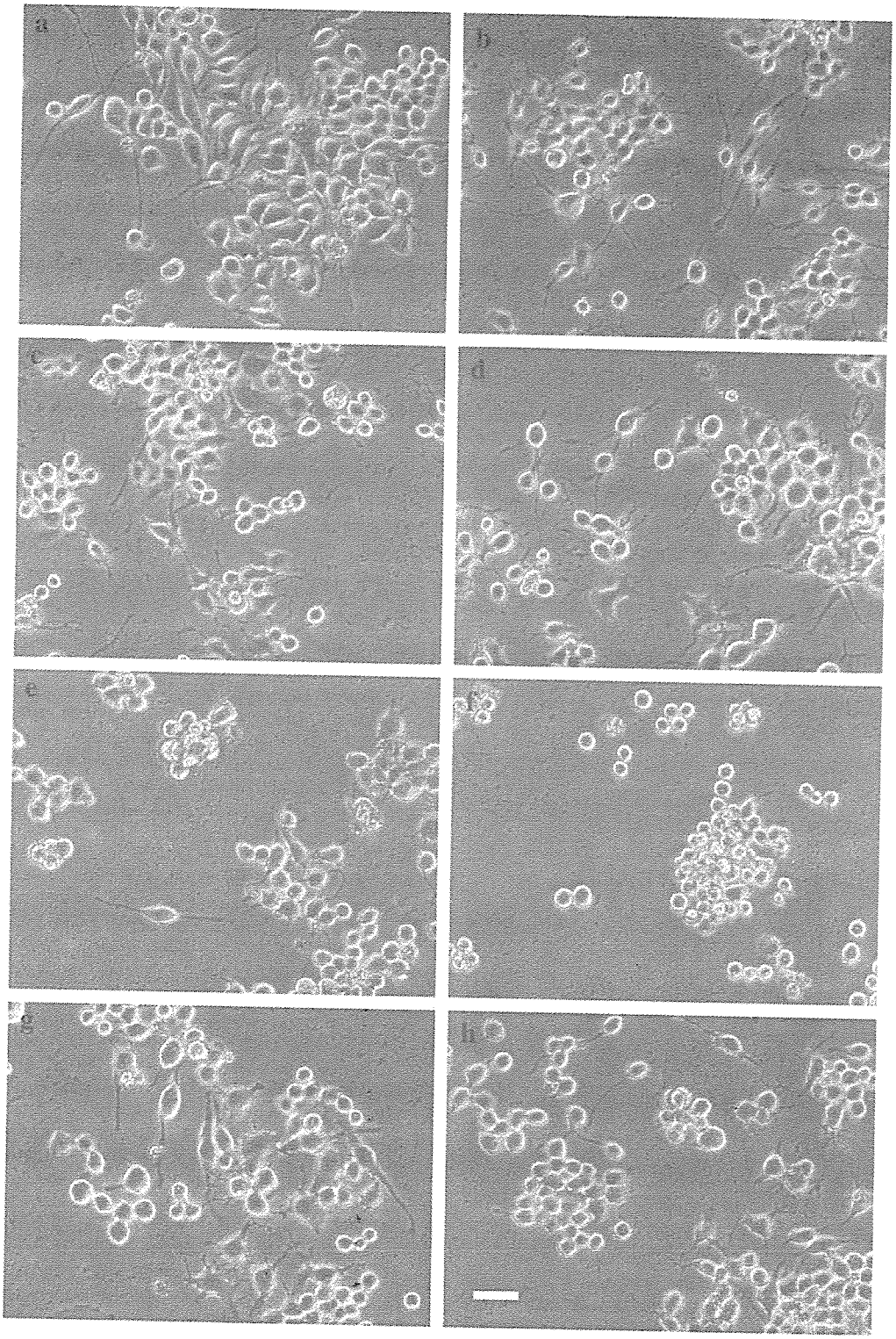

Fig. 3. Morphological differentiation of N2a cells with knockdown of *App*, *Aplp1* and *Aplp2*. Transfection of siRNA duplexes into N2a cells was carried out as described for Fig. 1. Twenty-four hours after transfection, culture medium was replaced with DMEM without serum, and further 24 h culture was carried out as described for Fig. 2. Transfected siRNA duplexes were as follows: (a) no siRNA (jetSI reagent alone); (b) siControl; (c) siApp-1; (d) siApp-2; (e) siAplp1-1; (f) siAplp1-2; (g) siAplp2-1; (h) siAplp2-2. Scale bar indicates 50 μm.

inhibition of target gene expression was induced by the siRNA duplexes.

Because N2a cells are differentiated by serum deprivation [the resultant cells exhibit differentiated morphology with long neuritic processes (Fig. 3a)] (Diaz-Nido et al., 1988), we investigated the morphological differentiation of N2a cells with knockdown of *App*, *Aplp1* and *Aplp2* under serum deprivation. Fig. 3 shows photographs of N2a cells treated with siRNA duplexes after 24 h culture in the absence of serum. Neurite outgrowth was examined based on cell body diameter (approximately 15 μm) and cells with extended neurites longer than two cell body diameters were judged to be differentiated. As shown in the figure, moderate levels of neurite outgrowth were observed in N2a cells undergoing gene silencing of *App* and *Aplp2*; in contrast, very little neurite outgrowth was seen in N2a cells with knockdown of *Aplp1*. In addition, based on the observation of transfected cells, it appears that knockdown of the *App* gene family also influences cell viability. To further confirm this observation, we examined cell viability by means of MTS assay. As shown in Fig. 4, the results indicate that: (i) N2a cells with knockdown of *Aplp1* exhibit significantly reduced viability under the present culture conditions, in both the presence and absence of serum; (ii) knockdown of *App* apparently decreases cell viability under serum deprivation, but does not significantly affect viability in the presence of serum; and (iii) knockdown of *Aplp2* in N2a cells has little influence on cell viability. Taken together with the results of Fig. 3, it is possible that the inhibition of neurite outgrowth may be associated with decreased cell viability in N2a cells with knockdown of *Aplp1*.

Previous studies of *App*, *Aplp1* and *Aplp2* knockout mice have suggested that *App* family members possess essential, but partially redundant, functions, and that they play important roles in normal brain development and early postnatal survival (Heber et al., 2000; Herms et al., 2004; von Koch et al., 1997). Of the *App* family members, *Aplp2* may have a key function, as $Aplp2^{-/-}App^{-/-}$ and $Aplp2^{-/-}Aplp1^{-/-}$ double knockout is postnatally lethal, while $App^{-/-}Aplp1^{-/-}$ double knockout mice are viable. However, $Aplp2^{-/-}$ single knockout mice appeared to be normal (von Koch et al., 1997), whereas $Aplp1^{-/-}$ single knockout mice exhibited postnatal growth deficit (Heber et al., 2000).

Based on the present observations, *Aplp1* rather than *Aplp2* appears to play an important role in Neuro2a cells. Because *Aplp1* is specifically expressed in the nervous system (Lorent et al., 1995), it is possible that *Aplp1* plays an essential role in the survival and differentiation of neuronal cells (at least N2a cells). The present and previous observations also suggest that different cells (tissues) may require different contributions by the *App* gene family. To further evaluate these possibilities, more extensive studies are required.

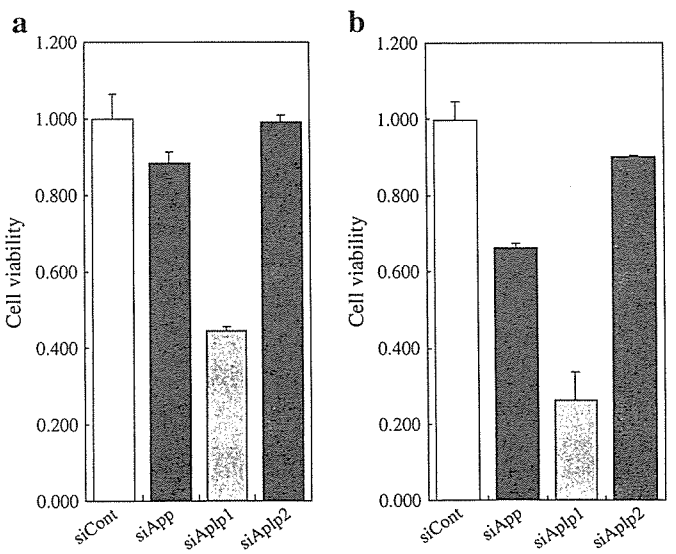

Fig. 4. Cell viability of N2a cells undergoing gene silencing of *App*, *Aplp1* and *Aplp2*. Transfection of siRNA duplexes was carried out as described for Fig. 1. Twenty-four hours after transfection, culture medium was replaced with DMEM with (A) or without (B) 10% serum. Seventy-two hours after transfection, cell viability was examined by means of MTS assay. Cell viability in the presence of siRNA duplexes against *App*, *Aplp1*, and *Aplp2* was normalized against that in the presence of siControl. Data are means of three independent experiments. Error bars represent standard deviations.

Acknowledgments

We would like to thank Y. Ohnishi and Y. Tamura for their helpful assistance. This work was supported in part by research grants from the Ministry of Health, Labor and Welfare of Japan.

References

Diaz-Nido J, Serrano L, Mendez E, Avila J. A casein kinase II-related activity is involved in phosphorylation of microtubule-associated protein MAP-1B during neuroblastoma cell differentiation. J Cell Biol 1988;106:2057–65.

Eggert S, Paliga K, Soba P, Evin G, Masters CL, Weidemann A, et al. The proteolytic processing of the amyloid precursor protein gene family members APLP-1 and APLP-2 involves alpha-, beta-, gamma-, and epsilon-like cleavages: modulation of APLP-1 processing by *n*-glycosylation. J Biol Chem 2004;279:18146–56.

Gu Y, Misonou H, Sato T, Dohmae N, Takio K, Ihara Y. Distinct intramembrane cleavage of the beta-amyloid precursor protein family resembling gamma-secretase-like cleavage of Notch. J Biol Chem 2001;276:35235–8.

Heber S, Herms J, Gajic V, Hainfellner J, Aguzzi A, Rulicke T, et al. Mice with combined gene knock-outs reveal essential and partially redundant functions of amyloid precursor protein family members. J Neurosci 2000; 20:7951–63.

Herms J, Anliker B, Heber S, Ring S, Fuhrmann M, Kretzschmar H, et al. Cortical dysplasia resembling human type 2 lissencephaly in mice lacking all three APP family members. EMBO J 2004;23:4106–15.

Hohjoh H. Enhancement of RNAi activity by improved siRNA duplexes. FEBS Lett 2004;557:193–8.

Li Q, Sudhof TC. Cleavage of amyloid-beta precursor protein and amyloid-beta precursor-like protein by BACE 1. J Biol Chem 2004;279:10542–50.

Lorent K, Overbergh L, Moechars D, De Strooper B, Van Leuven F, Van den Berghe H. Expression in mouse embryos and in adult mouse brain of three members of the amyloid precursor protein family, of the alpha-2-macroglobulin receptor/low density lipoprotein receptor-related protein and of its ligands apolipoprotein E, lipoprotein lipase, alpha-2-macroglobulin and the 40,000 molecular weight receptor-associated protein. Neuroscience 1995;65:1009–25.

Ohnishi Y, Tokunaga K, Kaneko K, Hohjoh H. Assessment of allele-specific gene silencing by RNA interference with mutant and wild-type reporter alleles. J RNAi Gene Silencing 2006;2:154–60.

Sago N, Omi K, Tamura Y, Kunugi H, Toyo-oka T, Tokunaga K, et al. RNAi induction and activation in mammalian muscle cells where Dicer and

eIF2C translation initiation factors are barely expressed. Biochem Biophys Res Commun 2004;319:50–7.

Scheinfeld MH, Ghersi E, Laky K, Fowlkes BJ, D'Adamio L. Processing of beta-amyloid precursor-like protein-1 and -2 by gamma-secretase regulates transcription. J Biol Chem 2002;277:44195–201.

Slunt HH, Thinakaran G, Von Koch C, Lo AC, Tanzi RE, Sisodia SS. Expression of a ubiquitous, cross-reactive homologue of the mouse beta-amyloid precursor protein (APP). J Biol Chem 1994;269:2637–44.

Turner PR, O'Connor K, Tate WP, Abraham WC. Roles of amyloid precursor protein and its fragments in regulating neural activity, plasticity and memory. Prog Neurobiol 2003;70:1–32.

von Koch CS, Zheng H, Chen H, Trumbauer M, Thinakaran G, van der Ploeg LH, et al. Generation of APLP2 KO mice and early postnatal lethality in APLP2/APP double KO mice. Neurobiol Aging 1997;18: 661–9.

Wasco W, Bupp K, Magendantz M, Gusella JF, Tanzi RE, Solomon F. Identification of a mouse brain cDNA that encodes a protein related to the Alzheimer disease-associated amyloid beta protein precursor. Proc Natl Acad Sci U S A 1992;89:10758–62.

Wasco W, Brook JD, Tanzi RE. The amyloid precursor-like protein (APLP) gene maps to the long arm of human chromosome 19. Genomics 1993a; 15:237–9.

Wasco W, Gurubhagavatula S, Paradis MD, Romano DM, Sisodia SS, Hyman BT, et al. Isolation and characterization of APLP2 encoding a homologue of the Alzheimer's associated amyloid beta protein precursor. Nat Genet 1993b;5:95–100.

Assessment of allele-specific gene silencing by RNA interference with mutant and wild-type reporter alleles

Yusuke Ohnishi[1,2], Katsushi Tokunaga[2], Kiyotoshi Kaneko[1] and Hirohiko Hohjoh[1,*]

[1]National Institute of Neuroscience, NCNP, 4-1-1 Ogawahigashi, Kodaira, Tokyo 187-8502, Japan; [2]Department of Human Genetics, Graduate School of Medicine, The University of Tokyo, 7-3-1 Hongo, Bunkyo-ku, Tokyo 113-0033, Japan

[*]*Correspondence to*: Hirohiko Hohjoh, *Email*: hohjohh@ncnp.go.jp, *Tel*: +81 42 342 2711, ext 5951, *Fax*: +81 42 346 1755

Journal of RNAi and Gene Silencing (2006), 2(1), 154-160

(Received 06 February 2006; Accepted 13 February 2006; Available online 28 February 2006; Published 28 February 2006)

ABSTRACT

Allele-specific gene silencing by RNA interference (RNAi) is therapeutically useful for specifically suppressing the expression of alleles associated with disease. To realize such allele-specific RNAi (ASP-RNAi), the design and assessment of small interfering RNA (siRNA) duplexes conferring ASP-RNAi is vital, but is also difficult. Here, we show ASP-RNAi against the Swedish- and London-type amyloid precursor protein (*APP*) variants related to familial Alzheimer's disease using two reporter alleles encoding the *Photinus* and *Renilla* luciferase genes and carrying mutant and wild-type allelic sequences in their 3'-untranslated regions. We examined the effects of siRNA duplexes against the mutant alleles in allele-specific gene silencing and off-target silencing against the wild-type allele under heterozygous conditions, which were generated by cotransfecting the reporter alleles and siRNA duplexes into cultured human cells. Consistently, the siRNA duplexes determined to confer ASP-RNAi also inhibited the expression of the *bona fide* mutant APP and the production of either amyloid β 40- or 42-peptide in Cos-7 cells expressing both the full-length Swedish- and wild-type *APP* alleles. The present data suggest that the system with reporter alleles may permit the preclinical assessment of siRNA duplexes conferring ASP-RNAi, and thus contribute to the design and selection of the most suitable of such siRNA duplexes.

KEYWORDS: *RNAi, allele-specific gene silencing, amyloid precursor protein, Swedish mutation, London mutation, reporter allele*

INTRODUCTION

RNA interference (RNAi) is a powerful tool for suppressing the expression of a gene of interest (Dykxhoorn et al, 2003; Meister and Tuschl, 2004; Mello and Conte, 2004). In mammals, RNAi can be induced by direct introduction of synthetic small interfering RNA (siRNA) duplexes into cells or generation of siRNA duplexes using short-hairpin RNA expression vectors and its application is expanding to various fields of science; therapeutic use of RNAi in medical science and pharmacogenesis is particularly promising (Caplen, 2004; Dykxhoorn et al, 2003; Hannon and Rossi, 2004; Karagiannis and El-Osta, 2005; Wood et al, 2003). Allele-specific gene silencing by RNAi (allele-specific RNAi: ASP-RNAi) is an advanced application of RNAi techniques, by which the expression of an allele of interest can be inhibited (Victor et al, 2002). Accordingly, ASP-RNAi is thought to be therapeutically useful, i.e., it can specifically suppress the expression of alleles causing disease without inhibiting the expression of corresponding wild-type alleles. To realize and control such ASP-RNAi, the following issues must be addressed: selection of competent siRNA duplexes that strongly induce ASP-RNAi; and qualitative and quantitative evaluation of allele-specific gene silencing.

In this article, we describe an easy assay system for assessment of ASP-RNAi with mutant and wild-type reporter alleles encoding the *Photinus* and *Renilla luciferase* genes. Using the amyloid precursor protein

(*APP*) variants (the Swedish- and London-type variants) related to familial Alzheimer's disease (Goate et al, 1991; Mullan et al, 1992) as model mutant alleles, we determined the effects of siRNA duplexes against the mutant *APP* on allele-specific silencing as well as off-target silencing against the wild-type allele. The siRNA duplexes having the potential to specifically suppress the expression of the mutant reporter allele consistently inhibited the expression of the *bona fide* mutant APP as well as amyloid β 40- and 42-peptides in Cos-7 cells expressing both the full-length Swedish- and wild-type *APP* alleles. These observations suggest that the present system could permit the selection of siRNA duplexes having the potential to confer ASP-RNAi.

MATERIALS AND METHODS

Preparation of oligonucleotides

DNA and RNA oligonucleotides were obtained from INVITROGEN and TAKARA, respectively. For preparation of duplexes, sense- and antisense-stranded oligonucleotides (20 μM each) were mixed and annealed as described previously (Hohjoh, 2002). The sequences of synthesized oligonucleotides are shown in Tables 1 and 2. Non-silencing siRNA duplex (siControl; Qiagen) was used as a negative control.

Cell culture

HeLa, T98G and Cos-7 cells were grown at 37°C in Dulbecco's modified Eagle's medium (Wako) supplemented with 10% fetal bovine serum (Sigma), 100 U/ml penicillin and 100 μg/ml streptomycin (Sigma) in 5% CO_2-humidified chamber. T98G cells (Registry No. IFO50295) were obtained from the Health Science Research Resources Bank.

Construction of reporter and expression plasmids

In order to construct plasmids carrying reporter alleles, the phRL-TK (Promega) and pGL3-TK (Ohnishi et al., 2005) plasmids encoding the *Renilla* and *Photinus* luciferase genes, respectively, both of which were driven by the same herpes simplex virus thymidine kinase (TK) promoter, were digested with Xba I and Not I, and were subjected to ligation with synthetic oligonucleotide duplexes corresponding to the Swedish-, London- and wild-type *APP* alleles (sequences of the oligonucleotides used are indicated in Table 1). The resultant plasmids carry allelic *APP* sequences in the 3'-untranslated regions (UTRs) of the luciferase genes (Figure 1A). Expression plasmids, $pAPP695_{WT}$ and $pAPP695_{SWE}$ encoding full-length cDNAs of the wild- and Swedish-type *APP* alleles, respectively, were kindly provided by Dr Tanahashi (Tanahashi and Tabira, 2001).

Transfection and reporter assay

The day before transfection, cells were trypsinized, diluted with fresh medium without antibiotics, and seeded into 24-well culture plates (approximately 0.5×10^5 cells/well). Cotransfection of synthetic siRNA duplexes with reporter plasmids was carried out using Lipofectamine 2000 transfection reagent (Invitrogen) according to the manufacturer's instructions, and to each well, 0.24 μg (40 nM) of siRNA duplexes, 0.2 μg of pGL3-TK-backbone plasmid, 0.05 μg of phRL-TK-backbone plasmid and 0.1 μg of pSV-β-Galactosidase control vector (Promega) were applied. Twenty-four hours after transfection, cell lysate was prepared and expression levels of luciferase and β-Galactosidase were examined by the Dual-Luciferase reporter assay system (Promega) and Beta-Glo assay system (Promega), respectively, according to the manufacturer's instructions. In the case of transfection of siRNA duplexes and expression plasmids ($pAPP695_{WT}$ and $pAPP695_{SWE}$) into Cos-7 cells, 0.4 μg of each plasmid and 0.24 μg of siRNA duplexes were applied. Forty-eight hours after transfection, culture media was collected and cell lysate was prepared.

Western blotting and ELISA

Culture media and cell lysate prepared from transfected Cos-7 cells were examined by western blotting as described previously (Lesne et al., 2003). Equal amounts of proteins were separated by SDS-PAGE and electrophoretically blotted onto PVDF membranes (Millipore). Membranes were blocked for 1 h in blocking solution (5 % (v/w) fat-free milk and 0.05 % (v/v) Tween-20 in PBS) and

Table 1. Synthetic DNA oligonucleotides

Name	Sequence (5'----------3')
ssAPPwt(Sw)	CTAGCATGCAGGAGATCTCTGAAGTGAAGATGGATGCAGAATTCCGACA
asAPPwt(Sw)	GGCCTGTCGGAATTCTGCATCCATCTTCACTTCAGAGATCTCCTGCATG
ssAPP(K670N-M671L)	CTAGCATGCAGGAGATCTCTGAAGTGAATCTGGATGCAGAATTCCGACA
asAPP(K670N-M671L)	GGCCTGTCGGAATTCTGCATCCAGATTCACTTCAGAGATCTCCTGCATG
ssAPPwt(Lo)	CTAGCATGCTGTCATAGCGACAGTGATCGTCATCACCTTGGTGATGCTGA
asAPPwt(Lo)	GGCCTCAGCATCACCAAGGTGATGACGATCACTGTCGCTATGACAGCATG
ssAPP(V717I)	CTAGCATGCTGTCATAGCGACAGTGATCATCATCACCTTGGTGATGCTGA
asAPP(V717I)	GGCCTCAGCATCACCAAGGTGATGATGATCACTGTCGCTATGACAGCATG
ssAPP(V717F)	CTAGCATGCTGTCATAGCGACAGTGATCTTCATCACCTTGGTGATGCTGA
asAPP(V717F)	GGCCTCAGCATCACCAAGGTGATGAAGATCACTGTCGCTATGACAGCATG
ssAPP(V717G)	CTAGCATGCTGTCATAGCGACAGTGATCGGCATCACCTTGGTGATGCTGA
asAPP(V717G)	GGCCTCAGCATCACCAAGGTGATGCCGATCACTGTCGCTATGACAGCATG

Table 2. Synthetic siRNAs used in this study. Sense- and antisense-stranded siRNA elements are indicated by '-ss' and '-as', respectively.

siRNAs against the Swedish *APP* mutant	
Name	**Sequence (5'----------3')**
si(T7/C8)-ss	AGUGAAUCUGGAUGCAGAAUUU
si(T7/C8)-as	AUUCUGCAUCCAGAUUCACUUU
si(T8/C9)-ss	AAGUGAAUCUGGAUGCAGAAUU
si(T8/C9)-as	UUCUGCAUCCAGAUUCACUUUU
si(T9/C10)-ss	GAAGUGAAUCUGGAUGCAGAUU
si(T9/C10)-as	UCUGCAUCCAGAUUCACUUCUU
si(T10/C11)-ss	UGAAGUGAAUCUGGAUGCAGUU
si(T10/C11)-as	CUGCAUCCAGAUUCACUUCAUU
si(T11/C12)-ss	CUGAAGUGAAUCUGGAUGCAUU
si(T11/C12)-as	UGCAUCCAGAUUCACUUCAGUU
si(T12/C13)-ss	UCUGAAGUGAAUCUGGAUGCUU
si(T12/C13)-as	GCAUCCAGAUUCACUUCAGAUU
siRNAs against the London *APP* mutants	
Name	**Sequence (5'----------3')**
si(A8)-ss	AGUGAUCAUCAUCACCUUGUU
si(A8)-as	CAAGGUGAUGAUGAUCACUUU
si(A9)-ss	CAGUGAUCAUCAUCACCUUUU
si(A9)-as	AAGGUGAUGAUGAUCACUGUU
si(A10)-ss	ACAGUGAUCAUCAUCACCUUU
si(A10)-as	AGGUGAUGAUGAUCACUGUUU
si(A11)-ss	GACAGUGAUCAUCAUCACCUU
si(A11)-as	GGUGAUGAUGAUCACUGUCUU
si(A12)-ss	CGACAGUGAUCAUCAUCACUU
si(A12)-as	GUGAUGAUGAUCACUGUCGUU
si(T8)-ss	AGUGAUCUUCAUCACCUUGUU
si(T8)-as	CAAGGUGAUGAAGAUCACUUU
si(T9)-ss	CAGUGAUCUUCAUCACCUUUU
si(T9)-as	AAGGUGAUGAAGAUCACUGUU
si(T10)-ss	ACAGUGAUCUUCAUCACCUUU
si(T10)-as	AGGUGAUGAAGAUCACUGUUU
si(T11)-ss	GACAGUGAUCUUCAUCACCUU
si(T11)-as	GGUGAUGAAGAUCACUGUCUU
si(T12)-ss	CGACAGUGAUCUUCAUCACUU
si(T12)-as	GUGAUGAAGAUCACUGUCGUU
si(G8)-ss	GUGAUCGGCAUCACCUUGGUU
si(G8)-as	CCAAGGUGAUGCCGAUCACUU
si(G9)-ss	AGUGAUCGGCAUCACCUUGUU
si(G9)-as	CAAGGUGAUGCCGAUCACUUU
si(G10)-ss	CAGUGAUCGGCAUCACCUUUU
si(G10)-as	AAGGUGAUGCCGAUCACUGUU
si(G11)-ss	ACAGUGAUCGGCAUCACCUUU
si(G11)-as	AGGUGAUGCCGAUCACUGUUU
si(G12)-ss	GACAGUGAUCGGCAUCACCUU
si(G12)-as	GGUGAUGCCGAUCACUGUCUU

were incubated with anti-APP antibody 22C11 (Chemicon) or anti-α-tubulin antibody DM1A (Sigma) followed by washing in PBS and further incubation with horseradish peroxidase-conjugated donkey anti-mouse IgG (Jackson ImmunoResearch Laboratories). Antigen-antibody complexes were visualized using ECL chemiluminescent reagent (Amersham). Levels of Aβ40 and Aβ42 production in culture media were examined by human/rat β amyloid 40 and 42 ELISA kits (Wako) according to the manufacturer's instructions.

RT-PCR

Total RNA extraction, including treatment with DNase I (Ambion) twice followed by reverse transcription, were carried out as described previously (Sago et al., 2004). The resultant cDNAs were examined by real-time (RT)-PCR using the ABI PRISM 7300 sequence detection system (Applied Biosystems) with a SYBER green PCR master mix (Applied Biosystems) according to the manufacturer's instructions. PCR primers used were as follows:

For detection of the *Renilla luciferase* transcript:

renilla-F; 5'-GTTCTTTTCCAACGCTATTG-3'
renilla-R; 5'-GAAGCTCTTGATGTACTTAC-3'

For detection of the *Photinus luciferase* transcript:

photinus-F; 5'-TTTGATATGTGGATTTCGAG-3'
photinus-R; 5'-ATCGTATTTGTCAATCAGAG-3'

RESULTS

Assessment of siRNAs in heterozygous model system

In this study, the Swedish- and London-type mutants of the *APP* gene, which are involved in familial Alzheimer's disease, were used as model mutant alleles. The Swedish- and London-type *APP* mutants carry double and single nucleotide substitutions, respectively, which are followed by amino acid substitutions (K670N-M671L in the Swedish APP; V717I, V717F or V717G in the London APP) (Goate et al, 1991; Mullan et al, 1992). The resultant amino acid sequences in the Swedish and London-type APPs are preferably digested by β- and γ-secretase, respectively, resulting in accumulation of Aβ40 and Aβ42 peptides, which are the key factors of Alzheimer's disease (Cai et al, 1993; Citron et al, 1992; Mattson, 2004; Suzuki et al, 1994).

Mutant and wild-type reporter alleles were constructed as described in Materials and Methods. The resultant reporter alleles (Figure 1A), synthetic siRNA duplex against the mutant allele and the *β-galactosidase* gene (control) were cotransfected into human cells. Note that the transfected cells are artificially heterozygous with the mutant and wild-type *APP* reporter alleles; thus, the effects of test siRNA duplexes on suppression of both the mutant and wild-type alleles can be simultaneously examined.

ASP-RNAi against the Swedish-type APP allele

When the *Renilla* and *Photinus luciferase* genes were regarded as the Swedish and wild-type reporter alleles, respectively, the effects of the si(T7/C8) - si(T12/C13) duplexes against the Swedish mutant on allele-specific gene silencing were examined in HeLa cells. The results

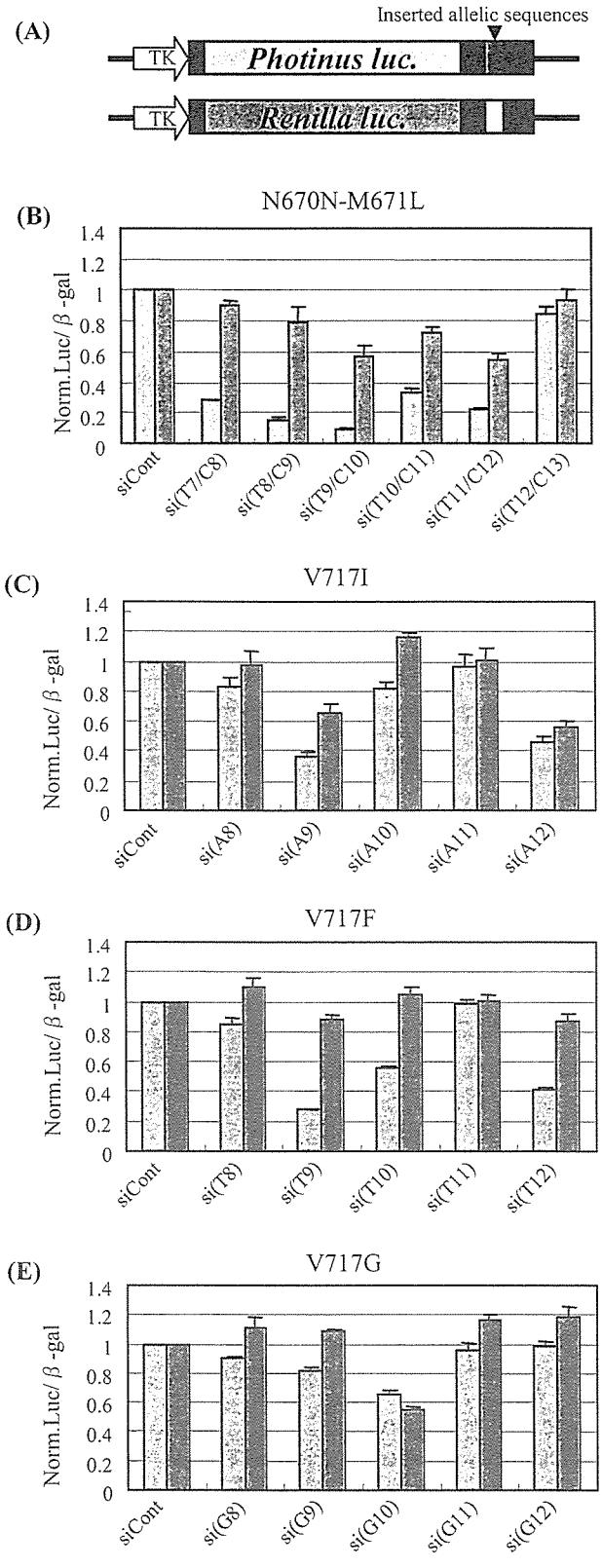

Figure 1. Assessment of ASP-RNAi with reporter alleles. (**A**) Schematic drawing of reporter alleles. Reporter alleles were constructed based on the *Photinus* and *Renilla luciferase* reporter genes driven by the same TK promoter, and allelic sequences of wild-type and mutant (synthetic oligonucleotides) were inserted into the 3'-UTRs of the reporter genes, i.e., the reporter alleles encode *luciferase* reporter genes carrying artificially inserted allele sequences of interest. Assessment of siRNA duplexes on the induction of ASP-RNAi against the Swedish *APP* mutant (**B**) and against the London APP mutants (**C-E**) was carried out. Synthetic siRNA duplexes against the mutants indicated were cotransfected with the mutant and wild-type reporter alleles and the *β-galactosidase* gene (control) into HeLa cells. The *Photinus* and *Renilla luciferase* genes carry the mutant and wild-type allelic sequences, respectively. Twenty-four hours after transfection, dual-luciferase and β-galactosidase assays were carried out. The levels of either *Photinus* (blue boxes) or *Renilla* (pink boxes) luciferase activity was normalized against the levels of β-galactosidase activity, and the ratios of mutant and wild-type luciferase activities in the presence of siRNA duplexes were normalized against the control ratio obtained in the presence of the siControl duplex (siCont). Data are averages of at least three independent determinations. Error bars represent standard deviations.

are shown in Figure 1B. The siRNA duplexes, except for the si(T12/C13) duplex, appeared to induce inhibition of mutant (*Photinus*) allele expression, while little or moderate inhibition of wild-type (*Renilla*) allele expression was seen, suggesting that the siRNA duplexes were able to discriminate the mutant reporter allele from the wild-type reporter allele. The si(T12/C13) duplex appeared to yield little or no RNAi activity. Considering the influence of the siRNA duplexes on the expression of the wild-type allele, the si(T8/C9) duplex appears to be the most suitable siRNA duplex conferring ASP-RNAi against the mutant allele. As for the si(T9/C10) and si(T11/12) duplexes inducing moderate levels of inhibition of wild-type allele expression, further analyses were carried out (Figure 4). Similar results were also obtained when the luciferase genes were exchanged between the mutant and wild-type reporter alleles, i.e., the *Photinus* and *Renilla luciferase* genes carried the wild-type and Swedish allele sequences, respectively (data not shown). In addition, when T98G cells, a human glioblastoma cell line, and Cos-7 cells were used instead of HeLa cells, results similar to those obtained in HeLa cells were observed (data not shown).

ASP-RNAi against London-type APP alleles

Because the London-type mutant possesses three types of single nucleotide change involved in amino acid substitution at position 717 (V717I, V717F and V717G), three mutant reporter alleles and corresponding wild-type reporter allele were constructed, and the effects of synthetic siRNA duplexes against the London-type mutants on suppression of the expression of either the target mutant allele or wild-type allele were examined under the present system. As shown in Figure 1C-E, various levels of gene silencing were observed and some of the siRNA duplexes, si(T9) and si(T12) (Figure 1D), appeared to discriminate the mutant alleles from the wild-type allele to some degree, resulting in ASP-RNAi; however, the other siRNA duplexes examined yielded less significant ASP-RNAi. Compared with the results for ASP-RNAi against the Swedish allele (Figure 1B), the induction and activation of ASP-RNAi against the London alleles appeared to be inferior to those against the Swedish mutant.

Western blot analyses of wild-type and Swedish APP in ASP-RNAi

We further investigated ASP-RNAi of siAPP duplexes against the Swedish mutant with full-length cDNAs of the Swedish and wild-type *APP* alleles, which were transiently

expressed in Cos-7 cells. The $pAPP695_{SWE}$ and/or $pAPP695_{WT}$ expression plasmids encoding full-length cDNAs of the Swedish and wild-type *APP* alleles, respectively, and siRNA duplexes targeting the Swedish mutant were cotransfected into Cos-7 cells, and expression of wild-type APP (APP_{WT}) and Swedish APP (APP_{SWE}) was examined by Western blotting. As shown in Figure 2, under homo(or hemi)zygous-like conditions, in which either APP_{WT} or APP_{SWE} was expressed, the signal intensity of $sAPP_{SWE}$ (secreted APP) and $cAPP_{SWE}$ (celluar APP) was apparently decreased in the presence of the si(T8/C9), si(T9/C10) and si(T11/C12) duplexes. In contrast, signals for either $sAPP_{WT}$ or $cAPP_{WT}$ were detected in the presence of any of the siRNA duplexes examined, which is consistent with the data for the reporter alleles described above. When APP_{SWE} and APP_{WT} were both expressed in the cells (heterozygous-like conditions), signals for APP were seen in the presence of any of the siRNA duplexes. Based on the results under homozygous-like conditions, the signals for APP in the presence of the si(T8/C9), si(T9/C10) and si(T11/C12) duplexes were most likely derived from APP_{WT}.

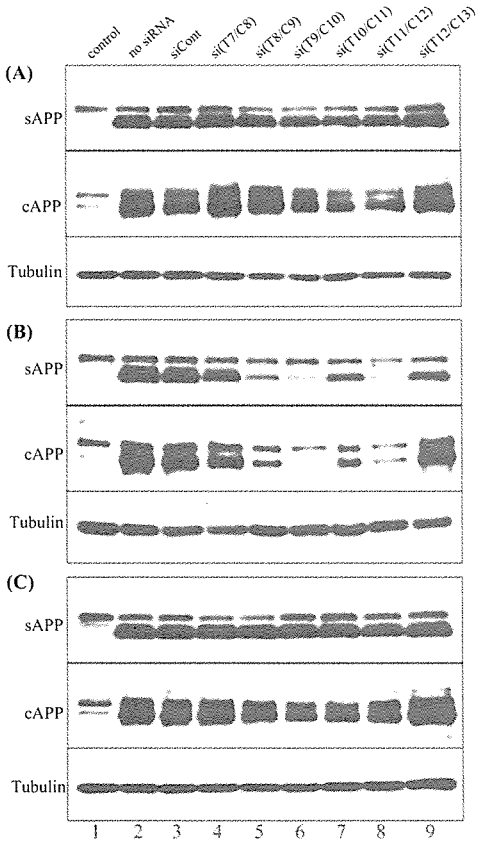

Figure 2. Expression of APP_{WT} and APP_{SWE} polypeptides under ASP-RNAi. Either the $pAPP695_{WT}$ (**A**) and $pAPP695_{SWE}$ (**B**) expression plasmids or the plasmids (**C**) together with the indicated siRNA duplexes against the Swedish mutant were introduced into Cos-7 cells, and expressed APP polypeptides in culture media (secreted APP: sAPP) and in cells (cellar APP: cAPP) were examined by Western blotting. Lane 1 (control) shows no transfected Cos-7 cells, in which endogenous APP is detectable. Lanes 2-9 are cells transfected with expression plasmid(s), and lanes 3-9 are cotransfected cells with the indicated siRNA duplexes. Expression of α-tubulin (control) is also shown.

The utility of ASP-RNAi using the siRNA duplexes assessed here in medical treatment can be demonstrated by confirming a significant decrease in Aβ peptides, which are a key factor in the development of Alzheimer's disease under heterozygous conditions expressing both APP_{SWE} and APP_{WT}. We thus determined the production levels of Aβ40 and Aβ42 peptides by means of ELISA. As shown in Figure 3, significant decreases in the production of either Aβ40 or Aβ42 peptide by RNAi (Figure 3A-C) and ASP-RNAi (Figure 3D-F) with the evaluated siRNA duplexes, particularly si(T8/C9), si(T9/C10) and si(T11/C12), was confirmed under homozygous and heterozygous conditions, respectively. Therefore, these results suggest the potential utility of such siRNA duplexes as therapeutic agents.

DISCUSSION

While ASP-RNAi is believed to be a useful technique, to realize and control ASP-RNAi, it is vital to design and select competent siRNA duplexes conferring ASP-RNAi; however, this is rather difficult without a procedure for assessing such siRNA duplexes. The system we present here could allow assessment, if designed siRNA duplexes have the potential for specifically inhibiting the expression of target alleles without suppressing the expression of other alleles. From a series of experiments with the Swedish- and London-type APP variants as model mutant alleles, we were able to determine potential siRNA duplexes for inducing ASP-RNAi. With regard to siRNA duplexes targeting the Swedish mutant, we further demonstrated that the si(T8/C9), si(T9/C10) and si(T11/C12) siRNA duplexes were able to significantly decrease the production of either Aβ40 or Aβ42 peptide in Cos-7 cells expressing both the full-length Swedish- and wild-type *APP* alleles. Accordingly, such competent siRNA duplexes conferring ASP-RNAi against mutant alleles likely hold utility as therapeutic agents.

In contrast to the Swedish mutant, there were difficulties in suppressing the London-type mutants carrying single nucleotide substitutions from the wild-type allele by ASP-RNAi. The difference between ASP-RNAi activities against the Swedish- and London-type mutants may have been caused by the number of base substitutions: the former and latter mutants carry double and single base substitutions, respectively. Another important point to note in the results for the London-type mutant is that different substitutions showed different ASP-RNAi activities, suggesting that the type of base change between the mutant and wild-type alleles could influence ASP-RNAi. With regard to the V717I (Figure 1C) and V717G (Figure 1E) mutants, a possible wobble base pair between siRNA and the wild-type mRNA (Du et al, 2005) and high GC content of siRNA used(Ui-Tei et al, 2004), respectively, might have negatively influenced the induction of ASP-RNAi; these possibilities require further examination in the future.

To further progress ASP-RNAi, it is necessary to design competent siRNA duplexes conferring strong allele-specific gene silencing. Chemical modifications (Chiu and Rana, 2003; Hall et al, 2004) and structural devices in siRNAs are considered to be applicable for improving

ASP-RNAi, and assessment of such siRNAs is feasible using the system we presented here. Altogether, it is suggested that the present assay system may contribute to the design and selection of the most suitable of siRNA duplexes conferring ASP-RNAi.

Finally, we add data indicating the possible inhibition of wild-type allele translation by the present siRNA duplexes. Because si(T9/C10) and si(T11/C12) exhibited moderate levels of inhibition of the expression of wild-type reporter allele (Figure 1B), we further investigated RNA levels of the wild-type allele by RT (real-time)-PCR. As shown in Figure 4, the levels of RNA expression of the wild-type allele in the presence of si(T9/C10) were similar to those in the presence of siControl, suggesting the possible inhibition of translation of the wild-type allele by the si(T9/C10) duplex. This may be due to a microRNA-like effect (Poy et al, 2004; Tang, 2005), and further study into this possibility remains necessary. With regard to the si(T11/C12) duplex, because a decrease trend in the levels of wild-type allele transcript was seen, it is possible that off-target gene silencing (Jackson et al, 2003) of the wild-type allele may occur in the presence of the duplex. Consequently, it is conceivable that the present system could further contribute to studies into off-target gene silencing and the function of microRNAs.

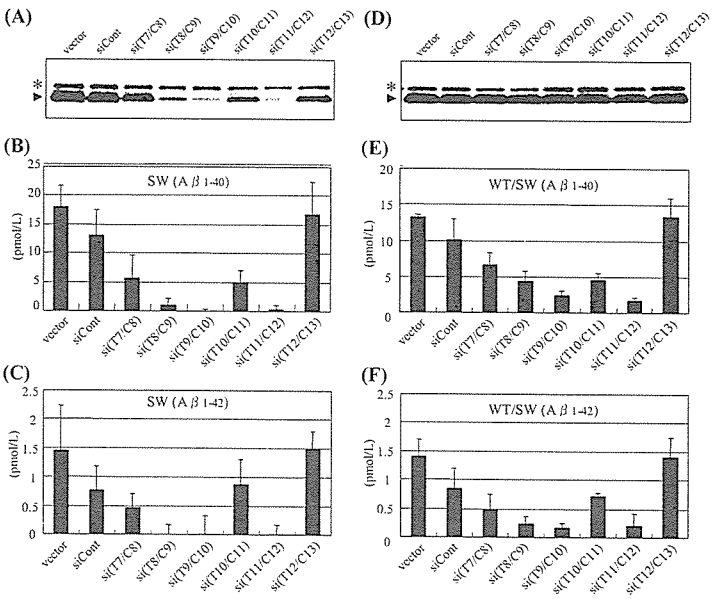

Figure 3. Production of Aβ40 and Aβ42 peptides under ASP-RNAi. The $pAPP695_{SWE}$ (**A-C**) plasmid and both the $pAPP695_{SWE}$ and $pAPP695_{WT}$ (**D-F**) plasmids together with the indicated siRNA duplexes against the Swedish mutant were cotransfected into Cos-7 cells, and expressed sAPP polypeptide and Aβ40 and Aβ42 peptides in culture media were examined by western blotting (**A, D**) and ELISA (**B, C, E, F**), respectively. "Vector" indicates cells transfected with only plasmid(s). Endogenous and exogenous (expressed) sAPPs are indicated by asterisks and arrow heads, respectively. ELISA data are averages of three independent determinations. Error bars represent standard deviations.

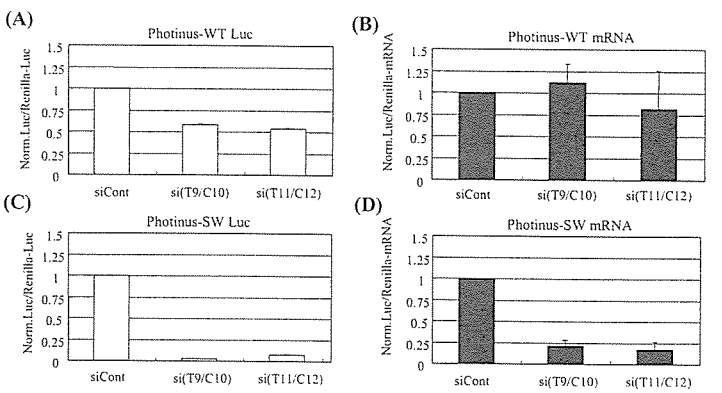

Figure 4. Possible translation inhibition and off-target silencing of wild-type reporter allele by siAPP duplexes. The si(T9/C10) or si(T11/C12) duplexes against the Swedish mutant allele together with either wild or mutant reporter allele plasmid carrying *Photinus luciferase* and the phRL-TK plasmid encoding *Renilla luciferase* (control) were introduced into HeLa cells. Twenty-four hours after transfection, dual-luciferase assay and isolation of total RNA were carried out. Off-target (to wild-type reporter allele) (**A**) and on-target (RNAi; to mutant reporter allele) (**C**) gene silencing were assessed based on luciferase activities. Ratios of normalized target (Photinus) luciferase activity to control (Renilla) luciferase activity are indicated: the ratios of luciferase activity determined in the presence of the si(T9/C10) or si(T11/C12) duplexes were normalized against the ratios obtained in the presence of the siControl duplex (siCont). Isolated RNAs in (**B**) and (**D**) corresponding to (**A**) and (**C**), respectively, were subjected to reverse transcription to